# A 30-Year Climatology of Northeastern U.S. Atmospheric Rivers

Anna N. Kaminski,<sup>a</sup> Jason M. Cordeira,<sup>b</sup> Nicholas D. Metz o <sup>c</sup> Katie Bachli,<sup>b</sup> Megan Duncan,<sup>b</sup> Michaela Ericksen,<sup>d</sup> Ivy Glade,<sup>e</sup> Cassandra Roberts,<sup>f</sup> and Clark Evans<sup>a</sup>

<sup>a</sup> Atmospheric Science Program, University of Wisconsin–Milwaukee, Milwaukee, Wisconsin
<sup>b</sup> Meteorology Program, Plymouth State University, Plymouth, New Hampshire
<sup>c</sup> Department of Geoscience, Hobart and William Smith Colleges, Geneva, New York
<sup>d</sup> Department of Atmospheric and Hydrologic Sciences, St. Cloud State University, St. Cloud, Minnesota
<sup>c</sup> Department of Earth Science, Minnesota State University–Mankato, Mankato, Minnesota
<sup>f</sup> Department of Environmental Science, Elizabethtown College, Elizabethtown, Pennsylvania

(Manuscript received 3 December 2021, in final form 18 October 2022)

ABSTRACT: Atmospheric rivers (ARs) are a frequently studied phenomenon along the West Coast of the United States, where they are typically associated with the heaviest local flooding events and almost one-half of the annual precipitation totals. By contrast, ARs in the northeastern United States have received considerably less attention. The purpose of this study is to utilize a unique visual inspection methodology to create a 30-yr (1988–2017) climatology of ARs in the northeastern United States. Consistent with its formal definition, ARs are defined as corridors with integrated vapor transport (IVT) values greater than 250 kg m<sup>21</sup> s<sup>21</sup> over an area at least 2000 km long but less than 1000 km wide in association with an extratropical cyclone. Using MERRA2 reanalysis data, this AR definition is used to determine the frequency, duration, and spatial distribution of ARs across the northeastern United States. Approximately 100 ARs occur in the northeastern United States per year, with these ARs being quasi-uniformly distributed throughout the year. On average, northeastern U.S. ARs have a peak IVT magnitude between 750 and 999 kg m<sup>21</sup> s<sup>21</sup>, last less than 48 h, and arrive in the region from the west to southwest. Average AR durations are longer in summer and shorter in winter. Further, ARs are typically associated with lower IVT in winter and higher IVT in summer. Spatially, ARs more frequently occur over the Atlantic Ocean coastline and adjacent Gulf Stream waters; however, the frequency with which large IVT values are associated with ARs is highest over interior New England.

KEYWORDS: Atmospheric river; Synoptic climatology; Synoptic-scale processes

#### 1. Introduction

An atmospheric river (AR) may be defined as a corridor of enhanced vertically integrated water vapor (IWV) and vertically integrated water vapor transport (IVT) within the warm sector of an extratropical cyclone ahead of a cold front (e.g., Ralph et al. 2004, 2017; Bao et al. 2006; Stohl et al. 2008; American Meteorological Society 2018). Regional and global case studies and climatologies often identify ARs using automated objective algorithms that query gridded meteorological data as a long (.2000 km) and narrow (,1000 km) corridor of IVT with magnitudes \$250 kg m<sup>21</sup> s<sup>21</sup> (Rutz et al. 2014); however, many different automated and numerical methods have been used to geometrically and/or phenomenologically identify ARs across the globe (e.g., Lavers and Villarini 2013; Shields et al. 2018). These differences in automated methods, which may or may not include all aspects of the aforementioned AR definition (e.g., association with an extratropical cyclone), may strongly influence studies that seek to relate ARs to both beneficial and hazardous outcomes related to

Kaminski's current affiliation: Department of Earth, Ocean, and Atmospheric Sciences, Florida State University, Tallahassee, Florida.

Corresponding author: N. D. Metz, nmetz@hws.edu

precipitation. The purpose of this study is to construct a 30-yr climatology of ARs over the northeastern United States (a region of the United States with a relative lack of AR-focused research) where visual inspection of multiple sources of climatological data may more accurately catalog different AR characteristics (e.g., spatial distribution, intensity, duration, and orientation) over the region.

Although included in global climatologies (e.g., Guan and Waliser 2019), the climatology of ARs over the central and eastern United States is comparatively less studied than ARs in the western United States (Slinskey et al. 2020). Those studies that do focus on ARs over the central and eastern United States are primarily impact-based analyses focusing on precipitation extremes and flooding over the central (e.g., Lavers et al. 2013; Nakamura et al. 2013; Rabinowitz et al. 2018), southeastern (e.g., Moore et al. 2015; Mahoney et al. 2016; Debbage et al. 2017; Miller et al. 2018), and northeastern (e.g., Hsu and Chen 2020; Sanders et al. 2020) United States. From a precipitation or impacts perspective across the northeastern United States, ;25% of non-summer precipitation is associated with ARs (Slinskey et al. 2020), .90% of non-summer extreme precipitation is associated with ARs (Slinskey et al. 2020), ; 50% of heavy or long-duration precipitation events are associated with either "pure" ARs or a "mixed/hybrid" type of events, and 95% of ice-jam events in New Hampshire occur in association with ARs (Sanders et al. 2020). From an AR perspective across the northeastern

United States, highly amplified large-scale flow patterns typically lead to landfalling ARs (Hsu and Chen 2020; Sanders et al. 2020) that are responsible for anomalously large precipitation events over the region (Hsu and Chen 2020).

The aforementioned analyses of ARs across the central and eastern United States also demonstrate that the characteristics of ARs in this region differ from those on the West Coast. For example, ARs, associated precipitation, and flooding are all more frequent in the western United States during November-April (Rutz et al. 2014) but are more frequent in the central United States during March-October (Lavers and Villarini 2013) while occurring in association with a similar fraction of extreme precipitation events (Slinskey et al. 2020). These analyses also suggest that IWV and IVT magnitudes in ARs over the southeastern and northeastern United States also tend to be higher on average than those that make landfall along the U.S. West Coast (e.g., Mahoney et al. 2016; Hsu and Chen 2020, respectively) likely supported by corridors of large water-vapor content directed from multiple warm-water sources including the Gulf of Mexico, the Caribbean Sea, the Atlantic Ocean, and the Gulf Stream (Mestas-Nuñez et al. 2007; Moore et al. 2013; Pfahl et al. 2014; Mahoney et al. 2016).

Additional motivation for the current study is provided by moisture and extreme precipitation that occurs due to or in association with ARs. Whereas a majority of precipitation in ARs is due to orographic precipitation in the western United States (e.g., Rutz et al. 2014), precipitation in ARs across the central and eastern United States occurs in conjunction with different processes (e.g., Teale and Robinson 2020), which may be influenced by the characteristics of the AR related to intensity, duration, or orientation to topographic barriers (e.g., Griffith et al. 2020). Case studies of AR-related precipitation across the United States suggest that the central and eastern United States are likely also influenced by 1) enhanced IWV lowering the environmental static stability and promoting vertical motion induced by frontogenesis and deep moist convection (e.g., Cannon et al. 2020), 2) enhanced IVT impinging upon mesoscale or other quasi-stationary boundaries (e.g., convective outflow; Moore et al. 2013), or 3) isentropic ascent along the associated cyclone's warm conveyor belt (e.g., Cordeira et al. 2013). These latter precipitation processes are more commonly found in or nearby ARs over the central and eastern United States where deep moist convection and warm conveyor belts (Madonna et al. 2014) are more common than over the West Coast. The likely prevalence of these different precipitation processes within large populations of ARs over the eastern United States is briefly discussed by Teale and Robinson (2020) but to date primarily only exist within case studies analyses.

This study focuses on quantifying the different characteristics of ARs related to spatial distribution, intensity, duration, and orientation over the lesser studied region of the northeastern United States. The northeastern United States is also selected in this study in part due to its proximity to the entrance of the North Atlantic storm track where cyclones and ARs may occur frequently, along with the potential for orographic, mesoscale, and synoptic-scale precipitation-related impacts across major metropolitan areas. The remainder of this paper is structured as follows. The data and methods used

in compiling the climatology are outlined in section 2. Climatological aspects of ARs in the northeastern United States are presented in section 3. Section 4 provides a summarizing discussion that contextualizes the results presented herein.

#### 2. Data and methods

This study focuses on developing a climatology of ARs over the northeastern United States extending from southwest to northeast from portions of West Virginia and Virginia to Maine. This region is the most densely populated region in the country with over 55 million people over 181 000 mi<sup>2</sup> (;469 000 km<sup>2</sup>) per the U.S. Census Bureau and includes elevated terrain of ;1-2 km along the northern Appalachian Mountains with a high point at Mount Washington, New Hampshire, of 1917 m. Here, the northeastern United States is approximated using a rectangular domain extending from 388N, 808W (along the central border between West Virginia and Virginia) to 488N, 668W (in the central portion of Chaleur Bay between the Canadian provinces of New Brunswick and Quebec; Fig. 1).

ARs over the northeastern United States are identified using a combination of criteria established by both Rutz et al. (2014) and the American Meteorological Society (2018) and include a corridor of IVT magnitudes \$250 kg m21 s21 that touches any portion of the Northeast domain, a corridor length \$2000 km, a corridor width of #1000 km, and spatially located in proximity to the cold front of an extratropical cyclone. Each of the candidate IVT corridors are tracked over time as they enter the domain, exist within the domain, and depart the domain. If these corridors meet the spatial and intensity criteria and are determined to be spatially located in proximity to the cold front of an extratropical cyclone at any point during their transit of the domain, they are recorded as an AR. These IVT corridors are also recorded as an AR if they are in proximity to stationary fronts trailing extratropical cyclones where the frontal boundary was previously or subsequently analyzed as a cold front. The study chose an IVT magnitude threshold of 250 kg m<sup>21</sup> s<sup>21</sup> to facilitate comparison with ARs along the U.S. West Coast. This value differs from Mahoney et al. (2016) who suggested an IVT magnitude threshold of 500 kg m21 s21 for ARs in the southeastern United States while investigating heavy precipitation. Other studies such as Guan and Waliser (2015), Guan et al. (2018), and Guan and Waliser (2019) use an IVT magnitude threshold that corresponds to a location's climatology (i.e., the greater of either the 85th percentile or 100 kg m<sup>21</sup> s<sup>21</sup>) to establish global AR chronologies used in studies such as Slinskey et al. (2020), but do not include criteria that it be linked to an extratropical cyclone. The results of this study are presented in comparison with results from all these past studies with suggested reasons for any differences, including a direct comparison of our results with similar results using the underlying data corresponding to the trio of Guan and coauthor studies mentioned above.

ARs and their parent extratropical cyclones are larger in scale than the domain used in this study, and the methodology therefore first identifies all ARs over the eastern United States and western North Atlantic Ocean (see Fig. 1) and

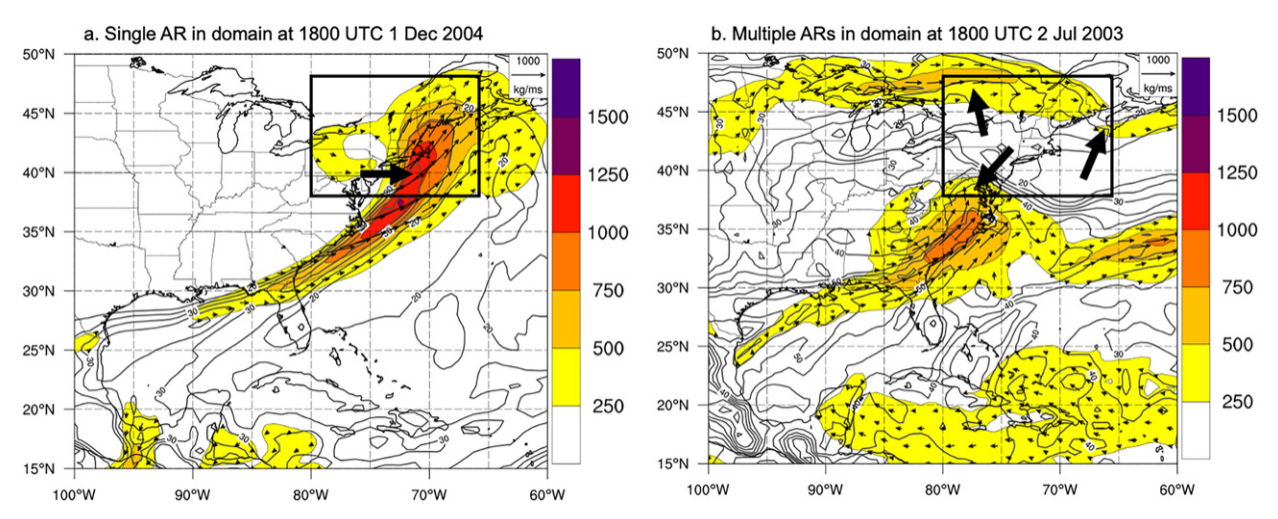


Fig. 1. Representative examples of (a) a single AR in the Northeast domain at 1800 UTC 1 Dec 2004 and (b) multiple ARs in the Northeast domain at 1800 UTC 2 Jul 2003, where dark-gray contours represent IWV (contoured every 5 mm starting at 20 mm), color shading represents IVT (kg m<sup>21</sup> s<sup>21</sup>), and vectors represent the magnitude and direction of the IVT (reference arrow in top right of each panel). The northeastern domain considered herein is outlined in black. Identified ARs are denoted by the black arrows. (Data source: NASA Merra-2 dataset.)

second determines whether each AR touches the Northeast domain. The IVT in this study is computed following the method of Neiman et al. (2008) every 6 h between 1 January 1988 and 31 December 2017 using the NASA MERRA-2 reanalysis (Gelaro et al. 2017). The objective AR identification criteria (IVT magnitude, length, and width) are applied manually to analyses every 6 h of MERRA2-derived IVT magnitude and direction spanning the 30-yr climatology on the eastern United States and western North Atlantic (i.e., the authors visually inspected 43 832 images). If visual inspection revealed an object (or objects) meeting the IVT magnitude, length, and width criteria over the eastern United States or western North Atlantic overlapped with the Northeast domain, it was subsequently cross referenced with archived surface analyses of North America from the NOAA Weather Prediction Center to confirm the object (or objects) as an AR located immediately ahead of a cold-frontal boundary or stationary front trailing an extratropical cyclone that could be previously or subsequently identified as a cold front. Note that all identified ARs only need to touch the Northeast domain to be considered herein. The maximum IVT magnitude (as 250-499, 500-749, 750-999, 1000-1249, 1250-1499, and \$1500 kg m<sup>21</sup> s<sup>21</sup>), duration (in 6-h increments), and IVT direction (visual approximation of the average over its lifetime within the domain as 1 of the 8 cardinal directions) were cataloged for confirmed ARs. Maximum IVT magnitude was used over some other measure given the visual nature of the identification.

## 3. Results

## a. General climatology

The study identified 3041 ARs within the northeastern U.S. domain during the 30-yr period, with an average of 101 ARs

per year and a standard deviation of 12.4 (Fig. 2a). The fewest number of ARs (N 5 69) occurred in 2013, and the largest number of ARs (N 5 131) occurred in 2017 (Fig. 2a). In any given month, there are on average 8.4 ARs over the northeastern U.S.

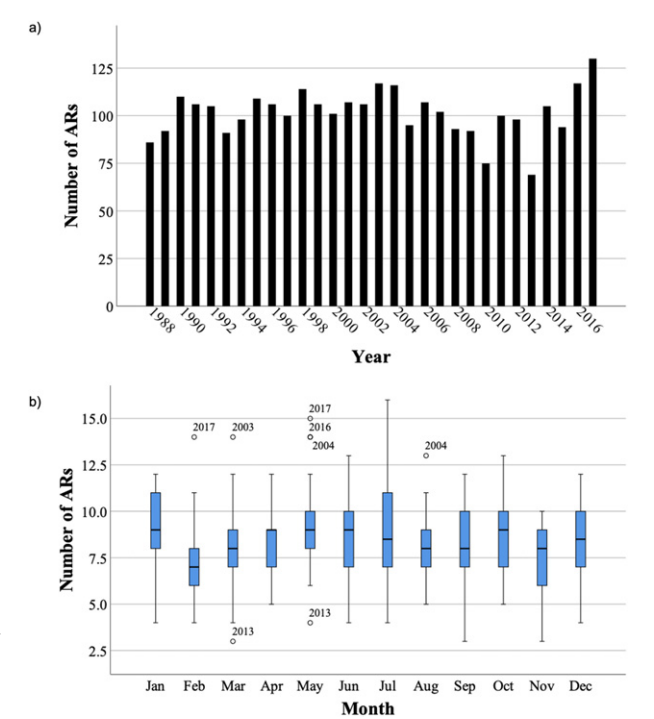
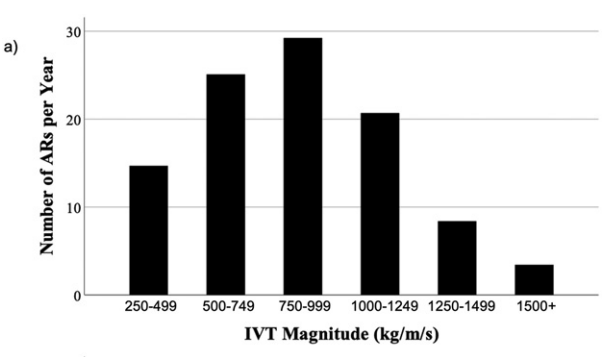


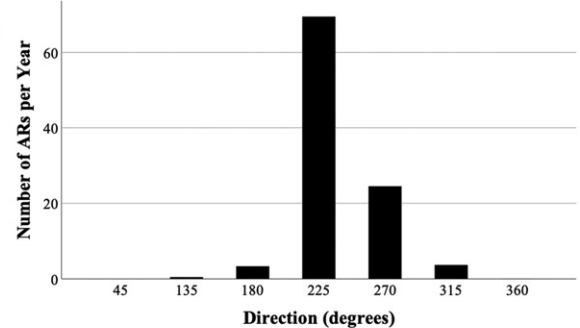
FIG. 2. (a) Total number of ARs recorded each year. (b) Boxand-whiskers plot of the total number of ARs by month, with the thick black line representing the mean, the box representing the 25th–75th percentiles, and the whiskers representing the minimum and maximum number of ARs in the data.

domain (Fig. 2b) with subtle variability among months (Fig. 2b). The value representing the mode of the distribution of maximum AR intensity within the northeastern U.S. domain was an IVT magnitude of 750-999 kg m<sup>21</sup> s<sup>21</sup>, representing 29% of all ARs followed by magnitudes of 500-749 kg m<sup>21</sup> s<sup>21</sup> (25%) and 1000-1249 kg m<sup>21</sup> s<sup>21</sup> (20%; Fig. 3a). Maximum IVT magnitudes within ARs over the Northeast U.S. domain \$ 1250 and \$ 1500 kg m21 s21 were comparatively rare (8% and 3%, respectively). A majority (61%) of ARs contained maximum IVT magnitudes \$ 750 kg m<sup>21</sup> s<sup>21</sup>, whereas a slightly larger majority (68.5%) of ARs in the Northeast U.S. domain also contained southwest IVT directions (2258 6 22.58), with an additional 24.1% of ARs favoring west IVT directions (2708 6 22.58) (Fig. 3b). A small minority of ARs contained south (3.3%), southeast (0.5%), or northwest (3.6%) IVT directions. The large number of ARs with southwest IVT directions is consistent with results presented by Slinskey et al. (2020), Hsu and Chen (2020), and Teale and Robinson (2020) for ARs over the northeastern United States; however, the mode of maximum IVT intensity \$ 750 kg m<sup>21</sup> s<sup>21</sup> is larger than the Slinskey et al. (2020) median value of ;500 kg m<sup>21</sup> s<sup>21</sup> and is similar to the Hsu and Chen (2020) spatial average 75th-percentile value of 700-800 kg m<sup>21</sup> s<sup>21</sup>. The average duration of an AR within the Northeast U.S. domain is 42.9 h, with a majority (64%) of ARs collocated with the domain for less than 48 h (Fig. 3c).

ARs with a maximum intensity of 750-999 kg m<sup>21</sup> s<sup>21</sup> are observed across all months (Fig. 4a). ARs with maximum intensities of 250-499 kg m<sup>21</sup> s<sup>21</sup> are relatively more common during December, January, and February, whereas ARs with maximum intensities of \$1000 kg m<sup>21</sup> s<sup>21</sup> are relatively more common during June-November (Fig. 4a). This seasonal distribution of AR intensity is likely related to seasonal variability in water vapor over the United States and the poleward and westward migration of the Bermuda high and maritime tropical air masses over the eastern United States during the warm season similar to results by Mahoney et al. (2016) and Hsu and Chen (2020). The poleward and westward migration of the Bermuda high also likely influences the IVT direction of ARs over the northeastern United States. Although southwest IVT directions in ARs are the most common throughout the year, the relative frequency of southwest IVT directions in ARs is lowest in the summer (Fig. 4b) giving way to a noticeable increase in west IVT directions in ARs during the warm season in line with summer versus autumnal composite mean differences in ARs studied by Hsu and Chen (2020). The higher intensity and more westerly ARs in summer also contain longer durations. These more-intense long-duration westerly ARs are likely associated with less progressive midlatitude flow patterns in summer as compared with less-intense shortduration southwesterly ARs in winter (Fig. 4c).

The size of the Northeast U.S. domain also yielded 765 times when there were multiple concurrent ARs (Fig. 5a). Multiple concurrent ARs occurred more frequently during 1998–2007, which also corresponded to an increase in the number of 6-h periods in which at least one AR was present over the northeastern United States (Figs. 5a,b). Note that a total number of 6-h periods of ;1000 (Fig. 5b) corresponds to





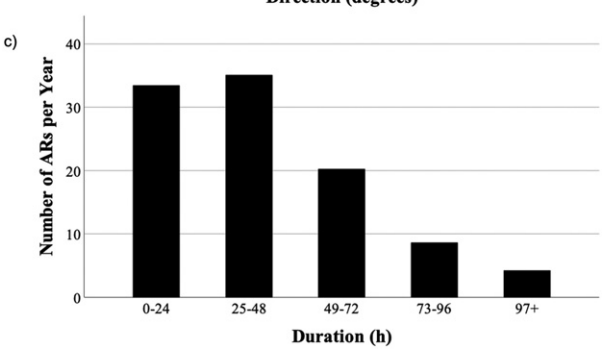


FIG. 3. Total number of ARs per year as a function of (a) peak IVT intensity (250–499, 500–749, 750–999, 1000–1249, 1250–1499, and \$1500 kg m $^{21}$  s $^{21}$ ), (b) direction (8, where 08 and 3608 5 from the north, 908 5 from the east, 1808 5 from the south, and 2708 5 from the west), and (c) duration in the Northeast domain (0–24, 25–48, 49–72, 73–96, and \$97 h).

;68% of the total 8760 h in a non-leap year. Given that the average AR persists in the domain for ;43 h, these numbers imply 1) an average frequency of ;140 ARs per year, which is higher than the average frequency in Fig. 2, and thus 2) that one or more ARs must exist simultaneously. The frequency of having one or more ARs over the northeastern United States is lowest in winter months and highest in summer months (Fig. 5c). We hypothesize that the prevalence of multiple concurrent ARs in summer may be due to the climatological poleward shift and weakening of the midlatitude westerlies over the United States allowing for more westerly and longer duration ARs (Figs. 4b,c) increasing the odds of overlapping events. The increase in frequency of multiple concurrent ARs in summer is responsible for a concomitant increase in the number of 6-h periods with an AR

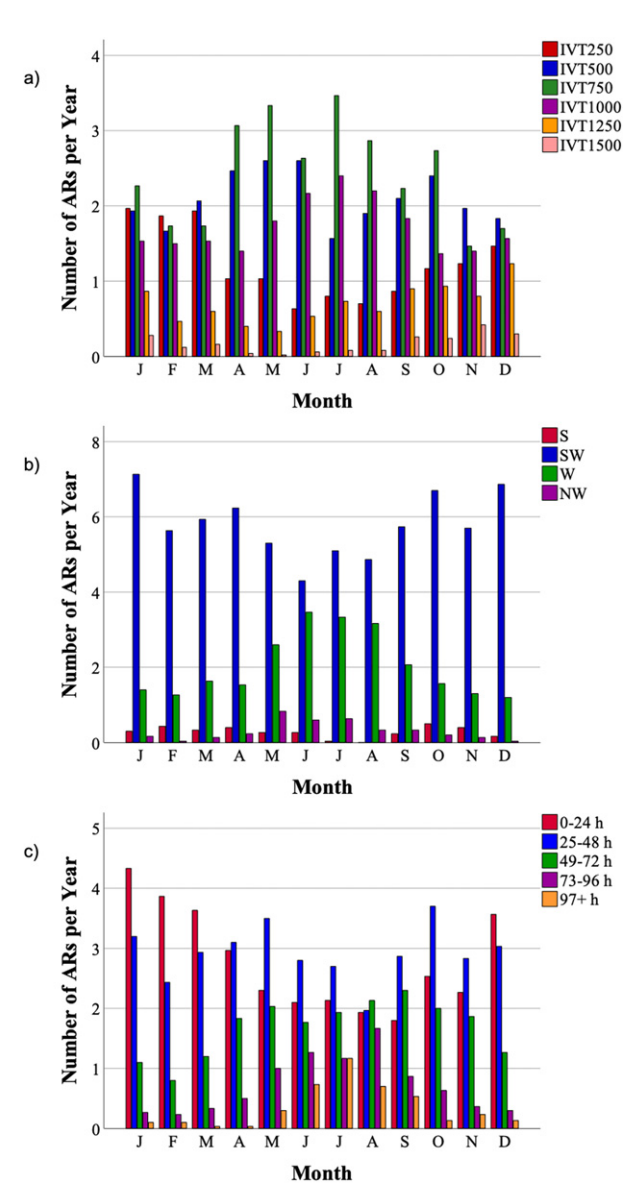


FIG. 4. Total number of ARs per year separated by month, including frequencies of (a) peak intensity (250–499, 500–749, 750–999, 1000–1249, 1250–1499, and \$1500 kg m<sup>21</sup> s<sup>21</sup>), (b) direction [from the south (S), from the southwest (SW), from the west (W), and from the northwest (NW)], and (c) duration in the Northeast domain (0–24, 25–48, 49–72, 73–96, and \$97 h).

present over the northeastern United States in summer months (Fig. 5d).

# b. Spatial climatology

The spatial frequency of ARs over the Northeast domain is illustrated via two analyses. The first analysis illustrates the frequency of IVT magnitudes \$250 kg m<sup>21</sup> s<sup>21</sup> at any given 6-h time when an AR was identified over the northeastern United States (Fig. 6a). This analysis demonstrates that ARs in the Northeast U.S. domain are present ;40% of the time over the Southeast corner of the domain proximal to the Gulf

Stream of the western North Atlantic Ocean and ;12%-18% in overland regions of New England (Fig. 6a). These overland and oceanic values are consistent with the frequency values over the northeastern United States and western North Atlantic Ocean presented by Slinskey et al. (2020) and Hsu and Chen (2020), respectively. The second analysis illustrates the likelihood that an AR was in the domain if a given location contained IVT magnitudes \$250 kg m<sup>21</sup> s<sup>21</sup> at any given 6-h time (Fig. 6b). This analysis demonstrates that a majority (;75%) of days with IVT magnitudes \$ 250 kg m<sup>21</sup> s<sup>21</sup> at any given grid point over New England are associated with ARs within the Northeast U.S. domain (Fig. 6b). This value is highest over the center of the domain where you would expect the frequency of ARs with predominantly southwest and westerly IVT directions to overlap. The location over the center of the domain also points to the potential impacts of low-level water vapor transport in the vicinity of the northern Appalachian Mountains, which could influence orographic precipitation depending on the orientation of IVT relative to the terrain.

These spatial analyses are partitioned into monthly distributions in order to show representative changes across seasons in January, April, July, and October in Figs. 7 and 8. Maxima in the spatial frequencies of IVT magnitudes \$ 250 kg m<sup>21</sup> s<sup>21</sup> when an AR was identified over the domain are largest in each month over the western North Atlantic Ocean, with values decreasing inland from the coast into northern New England and southeast Canada (Fig. 7). Overland maximum frequencies occur in July (;30%) and minimum frequencies occur in January (,10%). Alternatively, the odds that an AR was identified over the domain if the IVT magnitude was above 250 kg m<sup>21</sup> s<sup>21</sup> approaches 100% in January and is ;60% in July (Fig. 8). These analyses demonstrate that ARs occur somewhat infrequently over the Northeast U.S. domain (e.g., ,30% of the time) in any given month and less so in the winter, but when enhanced IVT is present over the domain, it is most likely associated with an AR, especially in winter.

### 4. Discussion and conclusions

This study presents a climatology of ARs that focuses on the northeastern United States, and documents AR frequency, intensity, duration, and spatial distribution. The ; 100 ARs over the northeastern United States per year contain an average maximum IVT magnitude of 750-999 kg m21 s21, IVT directions that are southwest or west, and persist over the domain for ;43 h on average (Fig. 3). During the cold season, ARs over the northeastern United States have comparatively lower maximum IVT magnitudes, a higher frequency of southwest IVT directions, and shorter durations, whereas warm-season ARs have higher maximum IVT magnitudes, a higher frequency of westerly IVT directions, and longer durations (Fig. 4). Although there is substantial variability in annual AR frequency (Fig. 2a), there is less variability in monthly AR frequency (Fig. 2b). Multiple concurrent ARs are more frequent, and the total number of 6-h periods with at least one AR in the region is higher in the summer as

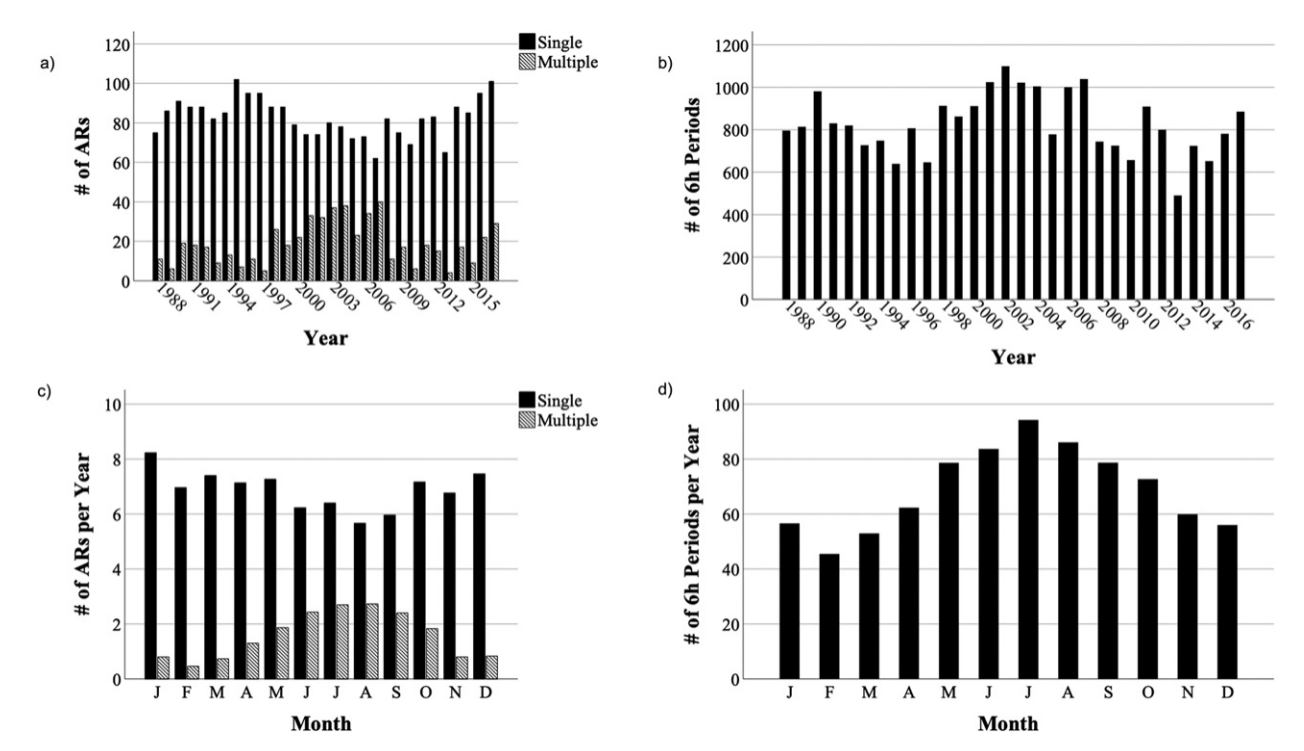
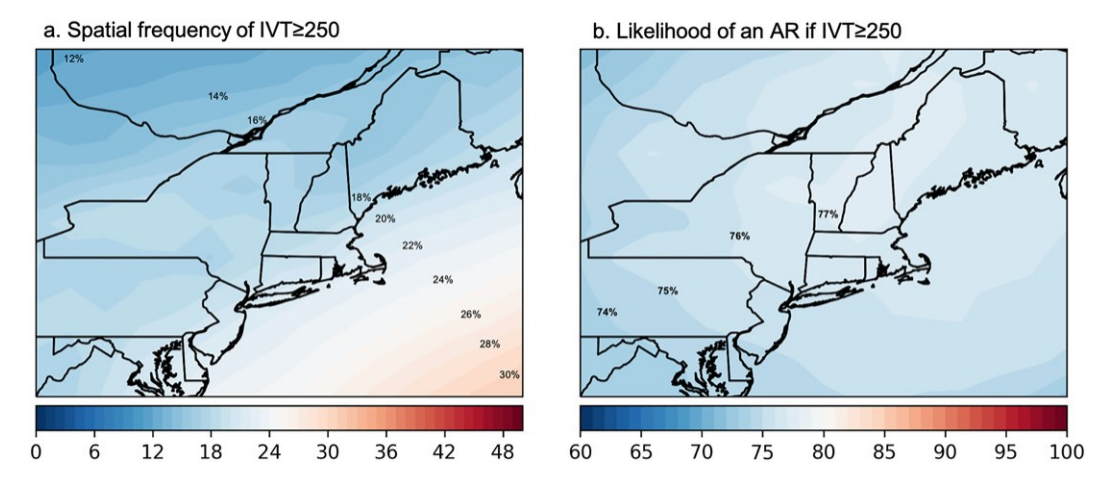


Fig. 5. The (a) annual and (c) monthly frequencies of ARs over the Northeast U.S. domain classified by when single ARs existed within the domain or multiple ARs existed within the domain. Also shown are the (b) annual and (d) monthly counts of 6-h periods when an AR existed within the domain.

compared with the winter (Figs. 5c,d). Spatially, ARs are more frequent over the adjacent Atlantic Ocean waters than over land, with frequency values that decrease farther inland toward Canada (Fig. 6a); however, IVT magnitudes \$ 250 kg m<sup>21</sup> s<sup>21</sup> at grid points over land are more likely to be associated with an AR than over nearby maritime regions (Fig. 6b). Note that the aforementioned substantial variability in AR frequency is likely driven by changes in the storm track

over eastern North America, which may be influenced by large-scale climate oscillations such as the El Niño-Southern Oscillation or quasi-biennial oscillation that are beyond the scope of the current study.

Prior to this study, Slinskey et al. (2020) considered climatological aspects of overland ARs in the northeastern United States as part of a broader study of ARs in each of the seven U.S. National Climate Assessment regions and



 $F_{IG}$ . 6. (a) Spatial frequency of IVT magnitudes \$250 kg m<sup>21</sup> s<sup>21</sup> when an AR was identified over the domain, and (b) the likelihood that an AR was identified over the domain if the IVT magnitude was above 250 kg m<sup>21</sup> s<sup>21</sup>. Note that the legend values differ between the two panels.

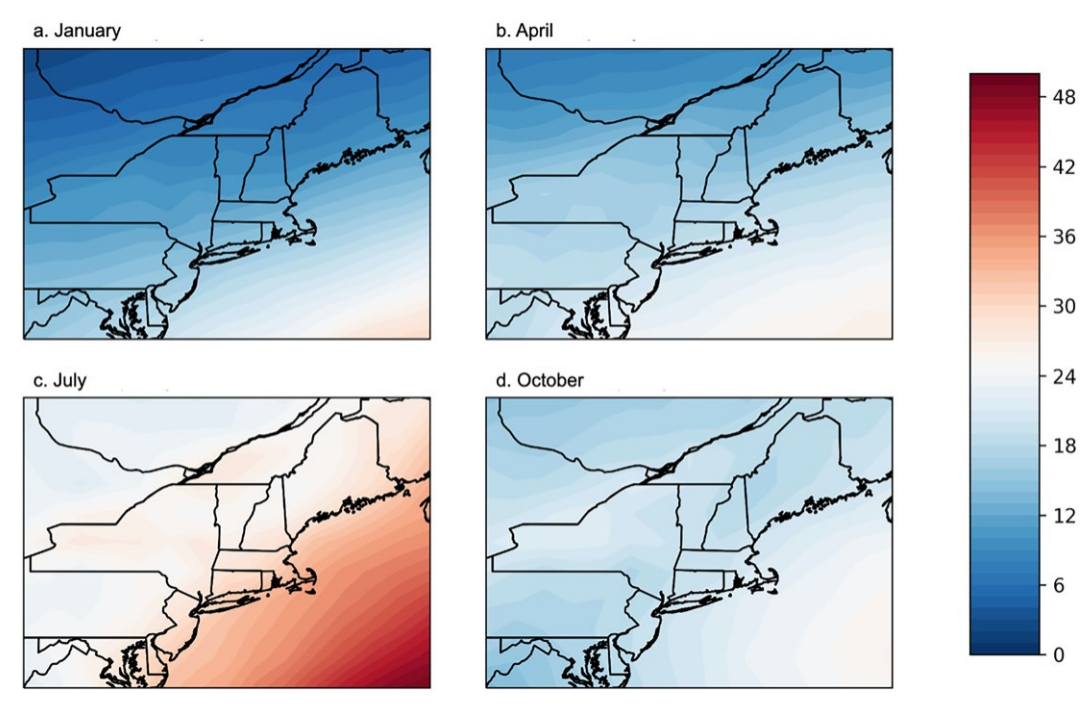


Fig. 7. Spatial frequency of IVT magnitudes \$250 kg m<sup>21</sup> s<sup>21</sup> when an AR was identified over the domain (as in Fig. 6a) for (a) January, (b) April, (c) July, and (d) October.

Hsu and Chen (2020) focused on circulation patterns associated with strong ARs over the "North American Northeast Coast." Although the three studies' results are broadly similar, there are some minor differences between the climatologies. For

instance, whereas Slinskey et al. (2020) suggest that ARs are most frequent in the northeastern United States in autumn, and Hsu and Chen (2020) in summer, this study found monthly frequencies that were rather constant and suggests

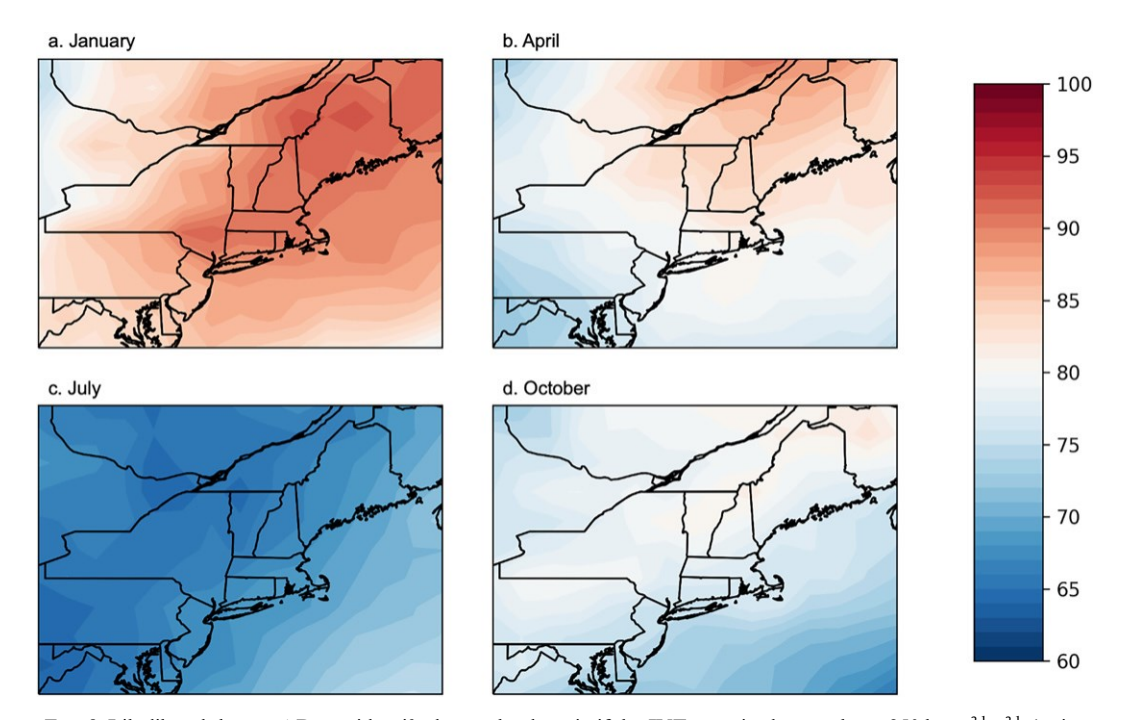


Fig. 8. Likelihood that an AR was identified over the domain if the IVT magnitude was above 250 kg m $^{21}$  s $^{21}$  (as in Fig. 6b) for (a) January, (b) April, (c) July, and (d) October.

that AR duration or occurrence of multiple concurrent events are more variable between seasons. This difference may result from the different methods used to identify ARs between studies. Whereas Slinskey et al. (2020) and Hsu and Chen (2020) use automated methods (e.g., Wick et al. 2013 or Guan and Waliser 2015) to identify ARs, this study 1) manually applied objective criteria to ensure that each AR is associated with extratropical cyclones using the North America surface analyses (and not with other phenomena) and 2) included nearby overwater grid points over the western North Atlantic [Slinskey et al. (2020) did not, but Hsu and Chen (2020) did]. The extra criteria to link ARs to their parent extratropical cyclone in this study are more in line with the AMS glossary definition of ARs and are not included in the aforementioned automated methods utilized by past studies of ARs over the eastern United States (e.g., Mahoney et al. 2016; Debbage et al. 2017; Hsu and Chen 2020; Slinskey et al. 2020). Further, whereas Slinskey et al. (2020) and Hsu and Chen (2020) quantified the AR footprint's median IVT magnitude and 75th-percentile IVT magnitude, respectively, this study quantified the AR peak magnitude in bins of 250 kg m<sup>21</sup> s<sup>21</sup>, thus resulting in the different IVT magnitudes reported among the studies.

Overall, ARs over the northeastern United States share similar characteristics to ARs documented elsewhere in the United States and the world. For example, there are typically more ARs in winter than in the summer along the U.S. West Coast (Waliser and Guan 2017), which is also true for the northeastern United States if multiple concurrent ARs during the summer are removed. On average, the typical AR along the U.S. West Coast has a duration of ; 20 h (Rutz et al. 2014; Ralph et al. 2019; Cordeira et al. 2019), whereas the typical AR over the northeastern United States has a duration of ;43 h (Fig. 3c), skewed by long duration ARs in the warm season. The daily average IVT magnitude of ARs along the U.S. West Coast is ;288 kg m<sup>21</sup> s<sup>21</sup>, which is substantially lower than the average peak IVT magnitude in the northeast at 750-999 kg m<sup>21</sup> s<sup>21</sup> (Fig. 3a). It is hard to directly compare these values given that the average magnitude along the U.S. West Coast was calculated as a daily average of IVT magnitudes while an AR was present, whereas over the northeastern United States it was calculated as the maximum IVT while an AR was present. Spatially, the Coastal Ranges, Cascades, and Sierra Nevada, with some exceptions, block the eastward extent of ARs along the U.S. West Coast (Rutz et al. 2014); whereas the Appalachian Mountains do not seem to have a similar effect on ARs over the northeastern United States because most ARs contain IVT directions that are parallel to the major axis of the terrain (from southwest to northeast). Outside the United States, AR frequencies and intensities in western Europe and the Iberian Peninsula are similar to those over the northeastern United States. For example, ARs are most frequent during the late autumn and winter seasons in western and central Iberia (Cortesi et al. 2014; Zêzere et al. 2014) and during the summer and early autumn in eastern Iberia (Cortesi et al. 2014; Ramos et al. 2015). Similarly, peak IVT magnitudes in northern Europe and the Iberian Peninsula average

 $450-650 \text{ kg m}^{21} \text{ s}^{21}$ , but only five cases recorded peak IVT magnitudes .  $900 \text{ kg m}^{21} \text{ s}^{21}$  (Ramos et al. 2015).

The visual inspection methodology used in this study identified a total of 3041 ARs over the Northeast domain with an average of ;101 per year. This methodology differs from other AR climatologies that use an algorithm-based objective identification methodology. The methodology also ensures that each candidate AR object over the eastern United States and western North Atlantic not only meets the objective intensity and geometry criteria but also ensures that it is spatially linked to the cold front of an extratropical cyclone and is a distinct AR from a potential second AR also in the domain, a common finding in this study. A purely objective reproduction of our methodology using the data from Guan and Waliser (2019) without the linkage to extratropical cyclones identifies 3834 candidate ARs (;128 per year). Further analysis indicated that the monthly frequencies of these candidate ARs were nearly identical during the cool season [e.g., 9.03 per year in our study vs 9.13 per year using Guan and Waliser (2019) in January] but were very different during the warm season [e.g., 9.00 per year in our study vs 13.93 per year using Guan and Waliser (2019) in July]. The qualifications linking ARs to extratropical cyclones and as potentially discrete features are apparently necessary in evaluating ARs over the eastern United States where AR-like features may exist in the broad southerly IVT on the western periphery of the climatological Bermuda high in the warm season or when one or more ARs may be embedded within large plumes of IVT magnitudes of \$250 kg m21 s21 climatological Bermuda high in the warm season (not shown).

This study improves our understanding of the frequency and intensity of ARs over the northeastern United States and highlights key aspects of the climatology that influence seasonal distributions such as 1) the propensity for multiple concurrent ARs during the summer and 2) the overwhelming majority of events that favor southwest or west IVT directions. The latter therefore suggests that upslope precipitation associated with a majority of ARs over the northeastern United States is not as likely as those that make landfall along the U.S. West Coast (e.g., Griffith et al. 2020); however, the minority of events that do feature southerly or southeast IVT directions (as those may interact more favorably with the region's terrain) may be of particular interest to impact-based decision support services and forecasting for extreme precipitation and flooding in the most densely populated region in the United States. The ingredients used to describe ARs are well-known ingredients used by meteorologists within the National Weather Service and Northeast U.S. River Forecast Center to forecast the potential for extreme precipitation and flooding across the region (e.g., Lapenta et al. 1995; J. Arnott, J. Dellicarpini, and D. Vallee, personal communications 2020). Future work is therefore under way to examine the potential impacts of ARs on precipitation and hydrology (precipitation totals, flooding hazards, etc.) in the region and how the characteristics of high-impact ARs

in the region differ from the average AR presented in this study.

Acknowledgments. This research was initially conducted as part of the 2018 and 2019 Northeast Partnership for Atmospheric and Related Sciences (NEPARS) REU program and completed by the first author at her home institution. This research was supported by NSF Awards AGS-1757009 and AGS-1757010 (for all authors except Evans). The AR data for the comparison of results with Guan and Waliser (2019) were provided by Bin Guan (https://ucla.box.com/ ARcatalog). Development of the AR detection algorithm and databases was supported by NASA. Any opinions, findings, and conclusions or recommendations expressed in this material are those of the author(s) and do not necessarily reflect the views of the National Science Foundation. The first author also received financial support from the University of Wisconsin-Milwaukee's Office of Undergraduate Research. Reviews from three anonymous reviewers greatly improved the quality of this paper.

Data availability statement. The 30-yr AR climatology is publicly available through Plymouth State University's Lamson Library Digital Collections. MERRA2 data used to create the 30-yr AR climatology are available from the NASA Goddard Earth Sciences Data and Information Services Center (https://disc.gsfc.nasa.gov/datasets?project=MERRA-2). Archived NOAA/Weather Prediction Center surface analyses used in creating the 30-yr AR climatology are available online (https://www.wpc.ncep.noaa.gov/archives/web pages/sfc/sfc archive.php).

#### REFERENCES

- American Meteorological Society, 2018: Atmospheric river. Glossary of Meteorology, http://glossary.ametsoc.org/wiki/Atmospheric\_river.
- Bao, J.-W., S. A. Michelson, P. J. Neiman, F. M. Ralph, and J. M. Wilczak, 2006: Interpretation of enhanced integrated water vapor bands associated with extratropical cyclones: Their formation and connection to tropical moisture. Mon. Wea. Rev., 134, 1063–1080, https://doi.org/10.1175/MWR3123.1.
- Battisti, D. S., D. J. Vimont, and B. P. Kirtman, 2019: 100 years of progress in understanding the dynamics of coupled atmosphere-ocean variability. A Century of Progress in Atmospheric and Related Sciences: Celebrating the American Meteorological Society Centennial, Meteor. Monogr., No. 59, Amer. Meteor. Soc., 8.1–8.57, https://doi.org/10.1175/AMSMONOGRAPHS-D-18-0025.1.
- Cannon, F., and Coauthors, 2020: Observations and predictability of a high-impact narrow cold-frontal rainband over Southern California on 2 February 2019. Wea. Forecasting, 35, 2083– 2097, https://doi.org/10.1175/WAF-D-20-0012.1.
- Cordeira, J. M., F. M. Ralph, and B. J. Moore, 2013: The development and evolution of two atmospheric rivers in proximity to western North Pacific tropical cyclones in October 2010. Mon. Wea. Rev., 141, 4234–4255, https://doi.org/10.1175/MWR-D-13-00019.1.
- } } , J. Stock, M. D. Dettinger, A. M. Young, J. F. Kalansky, and F. Martin Ralph, 2019: A 142-year climatology of Northern

- California landslides and atmospheric rivers. Bull. Amer. Meteor. Soc., 100, 1499–1509, https://doi.org/10.1175/BAMS-D-18-0158.1.
- Cortesi, N., J. C. Gonzalez-Hidalgo, R. M. Trigo, and A. M. Ramos, 2014: Weather types and spatial variability of precipitation in the Iberian Peninsula. Int. J. Climatol., 34, 2661–2677, https://doi.org/10.1002/joc.3866.
- Debbage, N., P. Miller, S. Poore, K. Morano, T. Mote, and J. M. Shepherd, 2017: A climatology of atmospheric river interactions with the southeastern United States coastline. Int. J. Climatol., 37, 4077–4091, https://doi.org/10.1002/joc.5000.
- Gelaro, R., and Coauthors, 2017: The Modern-Era Retrospective Analysis for Research and Applications, version 2 (MERRA-2). J. Climate, 30, 5419–5454, https://doi.org/10.1175/JCLI-D-16-0758.1.
- Griffith, H. V., A. J. Wade, D. A. Lavers, and G. Watts, 2020: Atmospheric river orientation determines flood occurrence. Hydrol. Processes, 34, 4547–4555, https://doi.org/10.1002/hyp.13905.
- Guan, B., and D. E. Waliser, 2015: Detection of atmospheric rivers: Evaluation and application of an algorithm for global studies. J. Geophys. Res. Atmos., 120, 12514–12535, https://doi.org/10.1002/2015JD024257.
- } } , and } } , 2019: Tracking atmospheric rivers globally: Spatial distributions and temporal evolution of life cycle characteristics. J. Geophys. Res. Atmos., 124, 12523-12552, https://doi. org/10.1029/2019JD031205.
- } } , and F. M. Ralph, 2018: An intercomparison between reanalysis and dropsonde observations of the total water vapor transport in individual atmospheric rivers. J. Hydrometeor., 19, 321–337, https://doi.org/10.1175/JHM-D-17-0114.1.
- Hsu, H.-H., and Y.-T. Chen, 2020: Simulation and projection of circulations associated with atmospheric rivers along the North American northeast coast. J. Climate, 33, 5673–5695, https://doi.org/10.1175/JCLI-D-19-0104.1.
- Lapenta, K. D., and Coauthors, 1995: The challenge of forecasting heavy rain and flooding throughout the eastern region of the National Weather Service. Part I: Characteristics and events. Wea. Forecasting, 10, 78–90, https://doi.org/10.1175/1520-0434 (1995)010,0078:TCOFHR.2.0.CO;2.
- Lavers, D. A., and G. Villarini, 2013: Atmospheric rivers and flooding over the central United States. J. Climate, 26, 7829– 7836, https://doi.org/10.1175/JCLI-D-13-00212.1.
- } } , R. P. Allan, G. Villarini, B. Lloyd-Hughes, D. J. Brayshaw, and A. J. Wade, 2013: Future changes in atmospheric rivers and their implications for winter flooding in Britain. Environ. Res. Lett., 8, 034010, https://doi.org/10.1088/1748-9326/8/3/034010.
- Madonna, E., H. Wernli, H. Joos, and O. Martius, 2014: Warm conveyor belts in the ERA-Interim dataset (1979–2010). Part I: Climatology and potential vorticity evolution. J. Climate, 27, 3–26, https://doi.org/10.1175/JCLI-D-12-00720.1.
- Mahoney, K., and Coauthors, 2016: Understanding the role of atmospheric rivers in heavy precipitation in the southeast United States. Mon. Wea. Rev., 144, 1617–1632, https://doi.org/10.1175/MWR-D-15-0279.1.
- Mestas-Nunez, A. M., D. B. Enfield, and C. Zhang, 2007: Water vapor fluxes over the intra-Americas Sea: Seasonal and interannual variability and associations with rainfall. J. Climate, 20, 1910–1922, https://doi.org/10.1175/JCLI4096.1.
- Miller, D. K., D. Hotz, J. Winton, and L. Stewart, 2018: Investigation of atmospheric rivers impacting the Pigeon River basin

- of the southern Appalachian mountains. Wea. Forecasting, 33, 283–299, https://doi.org/10.1175/WAF-D-17-0060.1.
- Moore, B. J., L. F. Bosart, D. Keyser, and M. L. Jurewicz, 2013: Synoptic-scale environments of predecessor rain events occurring east of the Rocky Mountains in association with Atlantic basin tropical cyclones. Mon. Wea. Rev., 141, 1022– 1047, https://doi.org/10.1175/MWR-D-12-00178.1.
- } } , K. M. Mahoney, E. M. Sukovich, R. Cifelli, and T. M. Hamill, 2015: Climatology and environmental characteristics of extreme precipitation events in the southeastern United States. Mon. Wea. Rev., 143, 718–741, https://doi. org/10.1175/MWR-D-14-00065.1.
- Nakamura, J., U. Lall, Y. Kushnir, A. W. Robertson, and R. Seager, 2013: Dynamical structure of extreme floods in the U.S. Midwest and the United Kingdom. J. Hydrometeor., 14, 485–504, https://doi.org/10.1175/JHM-D-12-059.1.
- Neiman, P. J., F. M. Ralph, G. A. Wick, J. D. Lundquist, and M. D. Dettinger, 2008: Meteorological characteristics and overland precipitation impacts of atmospheric rivers affecting the west coast of North America based on eight years of SSM/I satellite observations. J. Hydrometeor., 9, 22–47, https:// doi.org/10.1175/2007JHM855.1.
- Pfahl, S., E. Madonna, M. Boettcher, H. Joos, and H. Wernli, 2014: Warm conveyor belts in the ERA-Interim dataset (1979–2010). Part II: Moisture origin and relevance for precipitation. J. Climate, 27, 27–40, https://doi.org/10.1175/JCLI-D-13-00223.1.
- Rabinowitz, J. L., A. R. Lupo, and P. E. Guinan, 2018: Evaluating linkages between atmospheric blocking patterns and heavy rainfall events across the north-central Mississippi River valley for different ENSO phases. Adv. Meteor., 2018, 1217830, https://doi.org/10.1155/2018/1217830.
- Ralph, F. M., P. J. Neiman, and G. A. Wick, 2004: Satellite and CALJET aircraft observations of atmospheric rivers over the eastern North Pacific Ocean during the winter of 1997/98. Mon. Wea. Rev., 132, 1721–1745, https://doi.org/10.1175/1520-0493(2004)132,1721:SACAOO.2.0.CO;2.
- } } , and Coauthors, 2017: Dropsonde observations of total integrated water vapor transport within North Pacific atmospheric rivers. J. Hydrometeor., 18, 2577–2596, https://doi.org/10.1175/JHM-D-17-0036.1.
- } } , J. J. Rutz, J. M. Cordeira, M. Dettinger, M. Anderson, D. Reynolds, L. J. Schick, and C. Smallcomb, 2019: A scale to

- characterize the strength and impacts of atmospheric rivers. Bull. Amer. Meteor. Soc., 100, 269–289, https://doi.org/10.1175/BAMS-D-18-0023.1.
- Ramos, A. M., R. M. Trigo, M. L. R. Liberato, and R. Tomé, 2015: Daily precipitation extreme events in the Iberian Peninsula and its association with atmospheric rivers. J. Hydrometeor., 16, 579–597, https://doi.org/10.1175/JHM-D-14-0103.1.
- Rutz, J. J., W. J. Steenburgh, and F. M. Ralph, 2014: Climatological characteristics of atmospheric rivers and their inland penetration over the western United States. Mon. Wea. Rev., 142, 905–921, https://doi.org/10.1175/MWR-D-13-00168.1.
- Sanders, M. C., J. M. Cordeira, and N. D. Metz, 2020: Hydrome-teorological characteristics of ice jams on the Pemigewasset River in central New Hampshire. J. Hydrometeor., 21, 2923–2942, https://doi.org/10.1175/JHM-D-20-0027.1.
- Shields, C. A., and Coauthors, 2018: Atmospheric river tracking method intercomparison project (ARTMIP): Project goals and experimental design. Geosci. Model Dev., 11, 2455–2474, https://doi.org/10.5194/gmd-11-2455-2018.
- Slinskey, E. A., P. C. Loikith, D. E. Waliser, B. Guan, and A. Martin, 2020: A climatology of atmospheric rivers and associated precipitation for the seven U.S. national climate assessment regions. J. Hydrometeor., 21, 2439–2456, https://doi.org/10.1175/JHM-D-20-0039.1.
- Stohl, A., C. Forster, and H. Sodemann, 2008: Remote sources of water vapor forming precipitation on the Norwegian west coast at 608N}A tale of hurricanes and an atmospheric river. J. Geophys. Res., 113, D05102, https://doi.org/10.1029/ 2007JD009006.
- Teale, N., and D. A. Robinson, 2020: Patters of water vapor transport in the eastern United States. J. Hydrometeor., 21, 2123–2138, https://doi.org/10.1175/JHM-D-19-0267.1.
- Waliser, D., and B. Guan, 2017: Extreme winds and precipitation during landfall of atmospheric rivers. Nat. Geosci., 10, 179– 183, https://doi.org/10.1038/ngeo2894.
- Wick, G. A., P. J. Neiman, and F. M. Ralph, 2013: Description and validation of an automated objective technique for identification and characterization of the integrated water vapor signature of atmospheric rivers. IEEE Trans. Geosci. Remote Sens., 51, 2166–2176, https://doi.org/10.1109/TGRS.2012.2211024.
- Zêzere, J. L., and Coauthors, 2014: DISASTER: A GIS database on hydro-geomorphologic disasters in Portugal. Nat. Hazards, 72, 503–532, https://doi.org/10.1007/s11069-013-1018-y.